AGU PUBLICATIONS

Paleoceanography

RESEARCH ARTICLE
10.1002/2015PA002911

Key Points:
- Late Jurassic ITCZ at midtemperate latitudes
- Kimmeridge Clay deposition (35°N to 54°N) was controlled by tropical climate
- Organic carbon and clay patterns support strong orbital contrasts in humidity

Supporting Information:
- Supporting Information S1
- Table S1

Correspondence to:
H. A. Armstrong,
h.a.armstrong@durham.ac.uk

Citation:
Armstrong, H. A., T. Wagner, L. G. Herringshaw, A. J. Farnsworth, D. J. Lunt, M. Harland, J. Imber, C. Loptson, and E. F. L. Atar (2016), Hadley circulation and precipitation changes controling black shale deposition in the Late Jurassic Boreal Seaway, *Paleoceanography*, *31*, 1041–1053, doi:10.1002/2015PA002911.

Received 3 DEC 2015
Accepted 5 JUL 2016
Accepted article online 14 JUL 2016
Published online 3 AUG 2016

Hadley circulation and precipitation changes controling black shale deposition in the Late Jurassic Boreal Seaway

Howard A. Armstrong[1], Thomas Wagner[2], Liam G. Herringshaw[1,3], Alexander J. Farnsworth[4], Daniel J. Lunt[4], Melise Harland[5], Jonathan Imber[1], Claire Loptson[4], and Elizabeth F. L. Atar[1]

[1]Department of Earth Science, Durham University, Durham, UK, [2]Lyell Centre, Heriot-Watt University, Edinburgh, UK, [3]Department of Geography, Environmental, and Earth Sciences, University of Hull, Hull, UK, [4]School of Geographical Sciences and the Cabot Institute, University of Bristol, Bristol, UK, [5]Getech, Leeds, UK

Abstract New climate simulations using the HadCM3L model with a paleogeography of the Late Jurassic (155.5 Ma) and proxy-data corroborate that warm and wet tropical-like conditions reached as far north as the UK sector of the Jurassic Boreal Seaway (~35°N). This is associated with a northern hemisphere Jurassic Hadley cell and an intensified subtropical jet which both extend significantly poleward than in the modern (July–September). Deposition of the Kimmeridge Clay Formation (KCF) occurred in the shallow, storm-dominated, epeiric Boreal Seaway. High-resolution paleo-environmental proxy data from the Kimmeridge Clay Formation (KCF; ~155–150 Ma), UK, are used to test for the role of tropical atmospheric circulation on meter-scale heterogeneities in black shale deposition. Proxy and model data show that the most organic-rich section (*eudoxus* to mid-*hudlestoni* zones) is characterized by a positive $\delta^{13}C_{org}$ excursion and up to 37 wt % total organic carbon (%TOC). Orbital modulation of organic carbon burial primarily in the long eccentricity power band combined with a clear positive correlation between %TOC carbonate-free and the kaolinite/illite ratio supports peak organic carbon burial under the influence of very humid climate conditions, similar to the modern tropics. This reinterpretation of large-scale climate relationships, supported by independent modeling and geological data, has profound implications for atmospheric circulation patterns and processes affecting marine productivity and organic carbon burial further north along the Boreal Seaway, including the Arctic.

1. Introduction

Black shales represent major perturbations in the global carbon cycle and are recurrent throughout the Phanerozoic. At the present day, organic carbon (OC)-rich sediments are largely absent from the shallow continental shelves, in marked contrast to the extensive deposits found in epeiric basins and on continental margins and shelves in the past. The challenge for understanding marine black shale distribution, thickness, and—importantly—internal variations in deep time is to better constrain the processes that controlled the location and variability of OC production and burial and their relationship with atmospheric circulation, ocean currents, and dynamic depositional conditions.

There is a general consensus that in shallow marine settings OC accumulated in oxygen-deficient water beneath a stratified water column and resulted from a complex interplay between productivity, preservation, and dilution [e.g., *Tyson*, 2001]. The relative contribution of each of these factors is debated but each is directly or indirectly linked to atmospheric circulation, through nutrient supply via fluctuations in continental weathering intensity, precipitation and runoff, wind-driven oceanic upwelling, and large-scale surface current systems [*Arthur and Sageman*, 1994]. A comprehensive assessment of the processes and feedback operating at $<10^6$ years based on sediment data is difficult and requires both climate simulations and consistent high-resolution geologic data from multiple locations [*Wagner et al*., 2013].

Previous research has proposed that the British sector of the Late Jurassic Boreal Seaway, which connected the Tethys Ocean with the proto-Arctic (Figure 1), was governed by subtropical climate conditions [*Sellwood and Valdes*, 2008]. Dry subtropical climate is determined by the position of the poleward/descending limb of the atmospheric Hadley cells, which for paleoclimates can only be constrained indirectly in the geological record through precipitation proxies. Further information on the principles of Hadley cell dynamics for the present day can be found in *Yin* [2005] and for the Mesozoic greenhouse climate in *Wagner et al*. [2013]. Studies for the

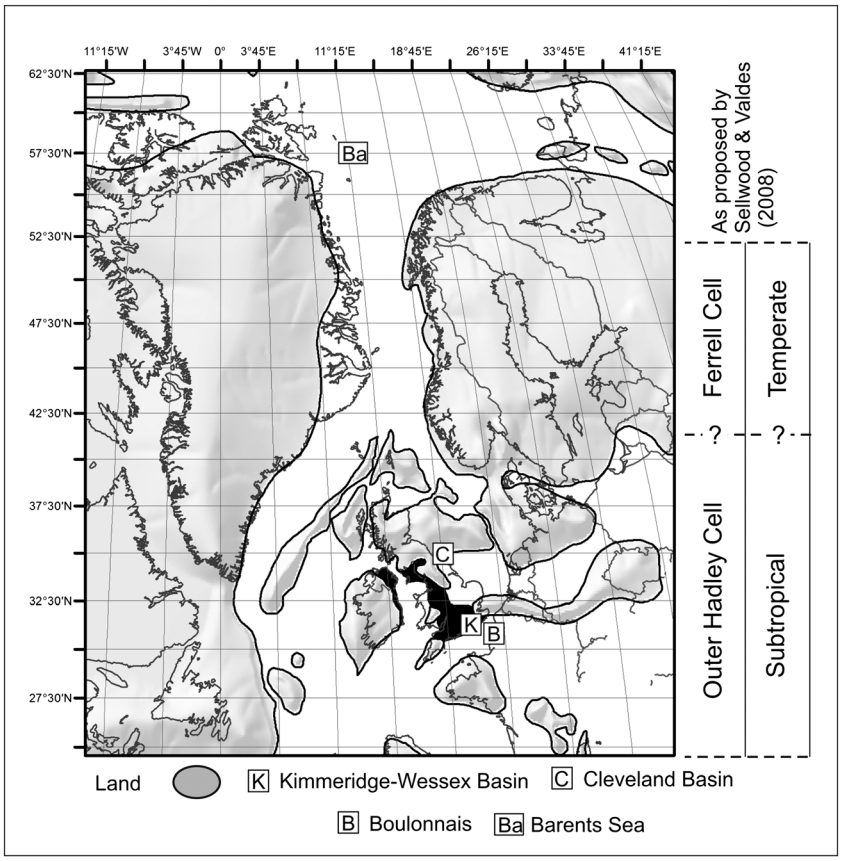

Figure 1. Paleogeography of NW Europe for the Kimmeridgian Stage (provided by Getech Group plc) including the sea level highstand line and the present-day countries rotated to their palaeopositions. The distribution of the Hadley cell and associated climate belts is based on previous work [*Sellwood and Valdes*, 2008], which we revise in this paper.

Cretaceous (highlighted below) provide some general insight on the dominant processes and feedback under the paleo-Hadley cells during global greenhouse conditions that may well also have operated in the Jurassic and during other time periods of global warmth:

1. Paleogeography affected the global large-scale atmospheric and marine circulation via modulations (strength and position) of the Hadley-Walker circulation and this affected regional precipitation [*Ohba and Ueda*, 2010].
2. Lower latitudinal temperature gradients and poleward expansion of the Hadley cells, with the descending, subtropical limbs located at around 25–30° [*Hay et al*., 2013].
3. Large latitudinal net moisture changes associated with an intensification of Hadley cell circulation [*Manabe and Bryan*, 1985].
4. A more vigorous terrestrial hydrological cycle leading to an increased nutrient flux to the oceans with implications for marine productivity and enhanced OC burial [*Hofmann and Wagner*, 2011].

The link between black shale formation and climate is long established [e.g., *Jenkyns*, 1980], and numerous studies have refined these connections and feedback and their biogeochemical consequences, particularly in open ocean basins [e.g., *Wagner et al*., 2013] and within the context of short-term global warming [*Jenkyns*, 2003]. It has been shown that seasonal to orbital-scale fluctuations in runoff, upwelling, productivity, and seawater redox can translate into black shales as millimeter- to meter-scale variations in OC content and quality [e.g., *Kuhnt et al*., 2005; *Wagner et al*., 2013], often linked with fluctuations in grain size and mineralogy [*Berger et al*., 1984]. These meter and submeter heterogeneities in shale can therefore be used to trace climate patterns during times of deposition and test for the links between orbitally modulated climate and OC deposition in the past.

Following the conceptual model developed for the subtropical-tropical Cretaceous Atlantic [*Wagner et al.*, 2013], the strongest contrasts in depositional conditions and geochemical properties, driven by orbitally paced wet/dry climate variations, occur beneath the ascending and descending limbs of the Hadley cell. Beneath the ascending limb, the forcing of nutrient flux via upwelling and monsoonal continental runoff is strongest, producing cycles of highly variable organic matter quantity and quality in the sedimentary record. Beneath the descending limb the influence of trade wind forcing produces continuous and generally enhanced OM quantity and quality [*Wagner et al.*, 2013]. The specific response of the Jurassic Hadley cell circulation to variable intensities and frequencies of orbital forcing and its impacts on deposition in epeiric basins, particularly at the regional scale, has not yet been tested on core material, defining the scope of this study on the Kimmeridge Clay Formation (KCF), primarily by using high-resolution data from sections in Dorset and Yorkshire, UK.

Our new climate simulations using the HadCM3L model with a paleogeography of the Late Jurassic (155.5 Ma [*Getech*, 2013]) indicate warm and wet tropical-like conditions between 35°N and 54°N during boreal summer (June–September) in the British sector of the KCF, previously described as "subtropical" [*Sellwood and Valdes*, 2008]. Our model is consistent with published high-resolution climate proxy data from the British sector of the KCF [*Desprairies et al.*, 1995; *Morgans-Bell et al.*, 2001; *Hesselbo et al.*, 2009; *Huang et al.*, 2010] that confirm a low-latitude climate control on OC productivity and deposition. We therefore expand the Cretaceous concept that at orbital time scales black shale deposition was directly linked to variation in rainfall intensity associated with the Hadley circulation [*Hofmann and Wagner*, 2011; *Wagner et al.*, 2013] to the Boreal Seaway of the Late Jurassic. If confirmed, this has fundamental implications for the climate and depositional controls and OC burial further north, into the proto-Arctic.

2. Geological Setting

Deposition of the KCF occurred during overall global greenhouse conditions with pCO_2 values at least 4 times higher than present atmospheric levels [*Sellwood and Valdes*, 2008]. Consistent with this global climate state, there is no direct geologic evidence for polar ice sheets at that time [*Dera et al.*, 2011]. There is a consensus that the KCF in the Wessex Basin of the UK was deposited in a shelf environment below fair-weather wave base but close to storm wave base [*Macquaker and Gawthorpe*, 1993]. Increasing organic (OC) content of the shales has been used as evidence for transgression during the lower part of the formation [see *Morgans-Bell et al.*, 2001]. Fluctuations in water column stratification and bottom water redox are indicated by sedimentology, ichnology and paleontology [*Wignall*, 1989; *Oschmann*, 1991], bulk organic and inorganic geochemistry [e.g., *Tyson et al.*, 1979], and biomarkers [*Sælen et al.*, 2000]. These independent lines of evidence support highly variable seawater redox conditions, from fully oxic to anoxic and euxinic. The presence of isorenieratene and its derivatives in samples from the *wheatleyensis* to *pectinatus* biozones indicates that the base of the photic zone was periodically euxinic [*Van Kaam-Peters et al.*, 1998].

3. Methods

The model simulations are run with the HadCM3L model, using the same configuration and spin-up procedure as in *Lunt et al.* [2016]. The model is run for a total of 1422 years, with a CO_2 concentration of 1120 ppmv, and a paleogeography of the Late Jurassic (155.5 Ma) including a sea level highstand line and topography defined using the methods of *Markwick and Valdes* [2004]. The final 30 years of the simulation are averaged to provide the climatologies. From these climatologies, we use an automated procedure to identify the Intertropical Convergence Zone (ITCZ), adapted from *Berry and Reeder* [2014]. Two methods of identification are used; the first is based on the maximum tropical precipitation (blue lines in Figure S2 in the supporting information), which identifies the ITCZ from its surface precipitation expression, and the second on the maximum midtropospheric (500 mbar) vertical velocity (red lines in Figure S2), which is a more dynamical definition based on the rapid ascent of buoyant air masses. We also identify subtropical zones using similar precipitation and vertical velocity metrics (black and orange lines in Figure S2). The automatically located ITCZ and subtropics for the Late Jurassic using the same identification method applied to modern conditions are shown in Figure S1. Based on these, and the precipitation maps themselves, we define the location of the ITCZ for the Late Jurassic in Figure 1 (red line).

We also identify global monsoonal regions during the Late Jurassic (Figure 3a) defined using the criteria of *Wang et al*. [2011], which uses the local summer minus winter precipitation rate that exceeds 2 mm/d with local summer precipitation also exceeding 55% of the annual total. Furthermore, we diagnose the modeled Jurassic large-scale atmospheric circulation, including Hadley cells, in terms of cross sections of the vertical and zonal (westerly) wind speeds (Figures 3b and 3c).

It is important to evaluate how well the model simulates the modern atmospheric circulation relative to observations. Our HadCM3L preindustrial simulation reproduces (Figure 3d) the spatial extent of the global monsoon regions from CPC Merged Analysis of Precipitation (CMAP; averaging period of 1979–2011) observations (Figure 3g) to a good degree. Furthermore, we test how well the model reproduces the large-scale circulation (vertical velocity (Figure 3e) and zonal wind (Figure 3f) latitudinal cross sections) between 169°W and 7.5°E (the longitudinal extent of the modern-day UK) against National Centers for Environmental Prediction (NCEP) Reanalysis v.2 (averaging period of 1979–2014; vertical velocity (Figure 3h) and zonal wind (Figure 3i) latitudinal cross sections); again, the model reproduces the main features to a good degree.

Linear sedimentation rates (LSR) and mass accumulation rates (MAR) of OC and bulk shale were calculated for each individual sedimentary cycle as defined by *Kuhnt et al.* [2005], assuming that (1) LSRs were linear within each sedimentary cycle and that (2) each of them represents one long eccentricity cycle of 400 kyr (Figure 4). The first assumption may well bear some inaccuracy in respect of short-term fluctuations in sedimentation and winnowing; however, we have no further evidence to improve this generalization. The second assumption is based on spectral analysis of % total organic carbon (TOC) [*Huang et al*., 2010]. To calculate bulk MARs dry bulk density (DBD) was used following $MAR_{bulk} = LSR*DBD$ with DBD obtained from the literature *Kuhnt et al*., 2005]. %TOC values are corrected for carbonate content using the following: TOC carbonate-free % = [100/(100-carbonate %)] * %TOC. The relationship between kaolinite/illite ratio and %TOC carbonate-free is based on data from Dorset [www.earth.ox.ac.uk/~rgge/data.html].

4. Results

4.1. Climate Simulations

Figure 2 and Figures S1 and S2 show the ITCZ as identified using the two criteria defined in the methods section. Contrary to the modern situation (for reference also shown in the supporting information), in June/July/August the ITCZ splits as it reaches the American continent from the east Pacific, resulting in a northern arm, which is pinned by the proto-Appalachian mountain range, and a southern arm, which is pinned by the North African mountain range. Of these, the northern arm is strongest and extends to about 30°N in the region of the KCF of the UK. The ITCZ is typically associated with the ascending branch of the Hadley circulation, found where vertical velocities are strongly negative from the surface to the top of the troposphere (units of Pa/s; blue regions in Figures 3b, 3e, and 3h) in the tropics. Typically, the stronger the vertical velocities through the atmosphere, the stronger the precipitation, because air converges at the surface in these regions, entraining moisture, and is then transported vertically. As the moist air is forced to rise, the moisture entrained condenses and precipitates out.

Figure 3b compared with Figure 3e supports the northward propagation of the ITCZ in the Kimmeridgian compared to the modern, shown by the maximum northward extension of the ascending arm of the northern hemisphere Hadley circulation (~35°N in August in the Kimmeridgian), although it also weakens compared to the modern. We also use zonal (westerly) wind profiles (units m/s) to indicate the position of large-scale wind features over the region of the paleo-UK for the Kimmeridgian simulation (Figure 3c), our preindustrial simulation (Figure 3f), and for present-day observations (Figure 3i). Of most interest is the position of the subtropical jet (STJ), a west-east flowing air current in the upper atmosphere. The STJ determines the maximum northward latitudinal extent of the Hadley circulation and thus the transport of moist-warm air from the equatorial regions northward. The STJ in Figures 3c, 3f, and 3i is indicated by positive values (m/s) at around 100–200 hPa in the atmosphere in the northerly latitudes (around 30–60°N typically). With the northward extension of the Hadley cell there is an associated $>15°$ northward migration in the STJ from ~35–40°N in June to ~55–60°N in August (Figure 3c compared with Figure 3f). This substantial northward movement of the STJ has a modern-day analogue in that the modern Indian monsoon system initializes once the STJ migrates northward of the Indian subcontinent. With the Boreal Seaway region in the simulation also being

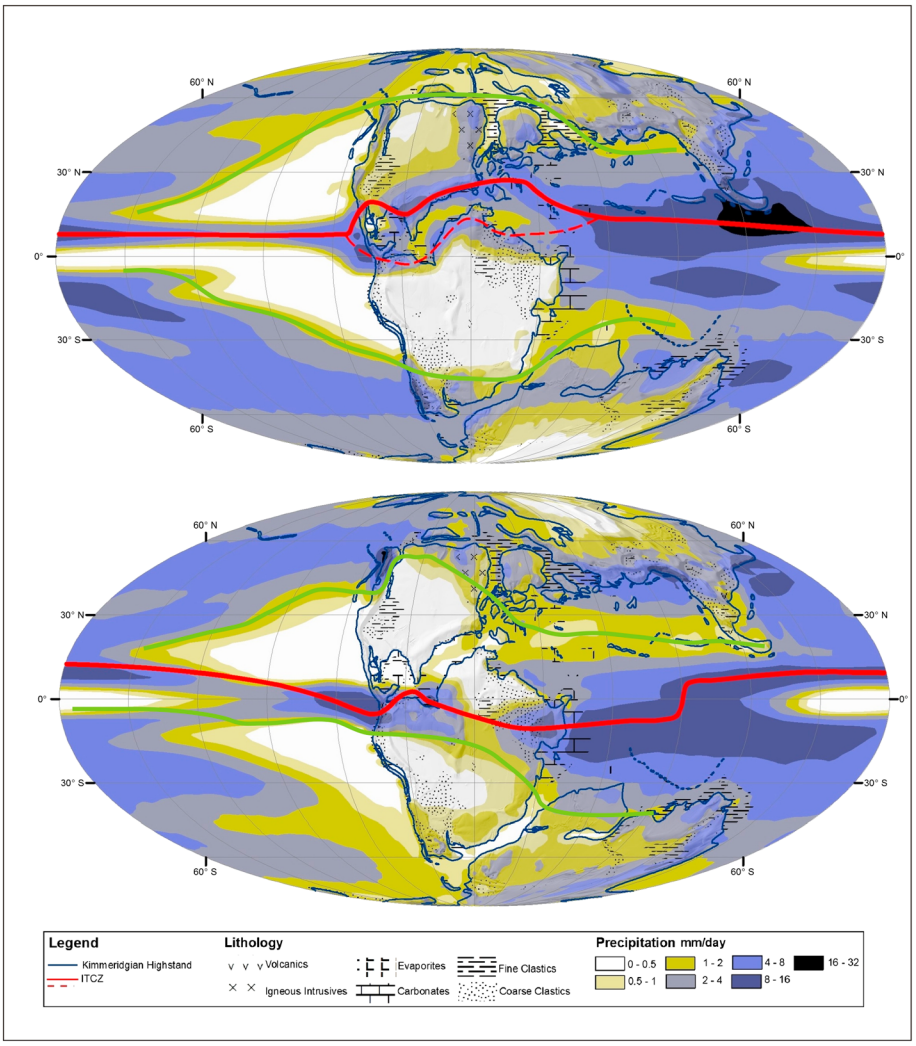

Figure 2. Modeled precipitation (contours, mm/d), location of the Intertropical Convergence Zone (ITCZ, red line) during the deposition of the KCF based on HadCM3L model and a paleogeography of the Late Jurassic (155.5 Ma [*Getech*, 2013]). Upper map is boreal summer (June, July, and August), and lower map is boreal winter (December, January, and February). During boreal summer the ITCZ lies in a more northerly location than at the present day placing the boreal sector of the NW European seaway temporarily under tropical-like conditions. The green line shows the approximate 1 mm/d precipitation contour, whose position is influenced by the location of the descending limb of the Hadley cell and the subtropical jet, as indicated in Figures 3b and 3c.

shown to be monsoonal (Figure 3a) we surmise that both a northward extension of the ITCZ and monsoonal conditions in the model will have had a strong influence on the Jurassic depositional environment.

Moving eastward, the ITCZ is then deflected southward into the tropical Tethys Ocean. Notably, the area of enhanced humidity is also pulled north on both sides of the NW European Boreal Seaway up to the Arctic Ocean, driven by elevated regions along the coastlines of Canada and Scandinavia. The character of the Indian and East Asian monsoons in the modeled Kimmeridgian had less continental precipitation compared to the modern. As for the modern, in December/January/February, the ITCZ is in the Southern Hemisphere, but the Jurassic ITCZ does not deflect as strongly over South America or Africa. Figure 2 and Figures S1 and S2 also show the location of the dry subtropical-like regions between 45 and 60°N, with the associated descending arm of the Hadley cell shown by the green line in Figure 2. This broadly parallels the ITCZ in the Northern Hemisphere. It extends across Laurentia into the paleo-Arctic Ocean in the vicinity of the Boreal Seaway and southward into central Europe-Asia. At least between 5.625 and 24.375°E longitudes and consistent with the subtropical jet core being centered around 55–60°N (Figure 3c).

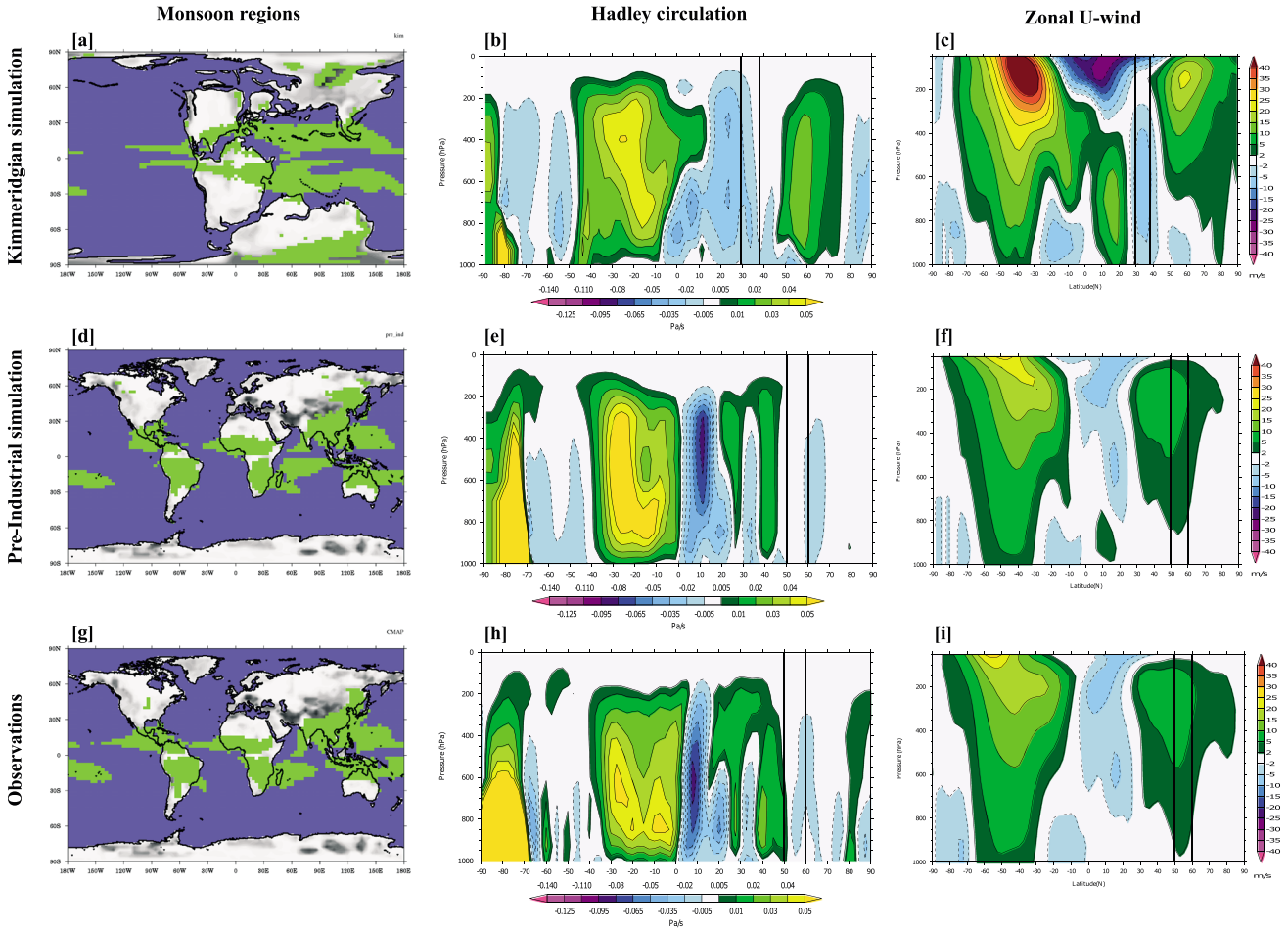

Figure 3. (a, d, and g) Global monsoon regions (highlighted in green) as defined by *Wang et al.* [2011] during the Late Jurassic (Kimmeridgian) simulation (Figure 3a), preindustrial simulation (Figure 3d), and for CMAP observations (Figure 3g), with topography shaded in grey. (b, e, and h) Latitudinal cross sections showing the August Hadley circulation, expressed as the atmospheric vertical velocity (Pa/s) for the longitude of the paleo-UK (paleo latitude 32.4°N, modern latitude 52°N), in the Kimmeridgian simulation (longitudinal mean 10.3°E–20.3°E; Figure 3b), preindustrial simulation (longitudinal mean 168.75°W–7.5°E; Figure 3e), and NCEP Reanalysis v.2 observations (longitudinal mean 168.75°W–7.5°E; Figure 3h). The Hadley circulation is a large-scale overturning atmospheric circulation. Ascending air from the surface to the top of the atmosphere (negative values, pascals/second, Pa/s, blue-pink colors) is associated with convergence at the surface. Descending air from the top of the atmosphere to the surface (positive values, green-yellow-orange colors) is associated with divergence at the surface. The ITCZ is typically centered in the region of large ascending (negative values) vertical velocities in the tropics. The black vertical lines depict the latitudinal extent of the modern UK and paleo-UK in the Kimmeridgian. (c, f, and i) Zonal (westerly) cross sections of atmospheric wind (m/s), for the longitude of the paleo-UK (paleo latitude 32.4°N, modern latitude 52°N), in the Kimmeridgian simulation (longitudinal mean 10.3°E–20.3°E; Figure 3c), preindustrial simulation (longitudinal mean 168.75°W–7.5°E; Figure 3f), and NCEP Reanalysis v.2 observations (longitudinal mean 168.75°W–7.5°E; Figure 3i). Here negative values (blue-pink colors) indicate wind traveling from east to west, while positive values (green-yellow-orange colors) indicate wind traveling from west to east. The black vertical lines depict the latitudinal extent of the modern UK and paleo-UK in the Kimmeridgian.

4.2. Sedimentology, Depositional Environment, and Astrochronolgy

Much of the Kimmeridge Clay Formation has a high OC content, but the most enriched interval occurs in the *wheatleyensis-hudlestoni* zones, where TOC frequently exceeds 10% [*Tyson*, 1996] (Figure 4). The depositional and preservational conditions during these specific periods are therefore of particular interest.

The three lithologies common to much of the formation—grey shale, black shale, and coccolith limestone—are present in the *wheatleyensis-hudlestoni* zones, suggesting that the depositional conditions were broadly similar to those interpreted elsewhere in the succession. The grey shales of the upper *wheatleyensis* zone are homogenized. This homogenization could have resulted from physical or biogenic (bioturbation) processes or a combination of the two. In the Clavell's Hard Stone Band, for example, occasional *Planolites* trace fossils are seen in homogeneous grey mudstone (Figure 5e), providing evidence that the sediment was being intensely processed by infauna.

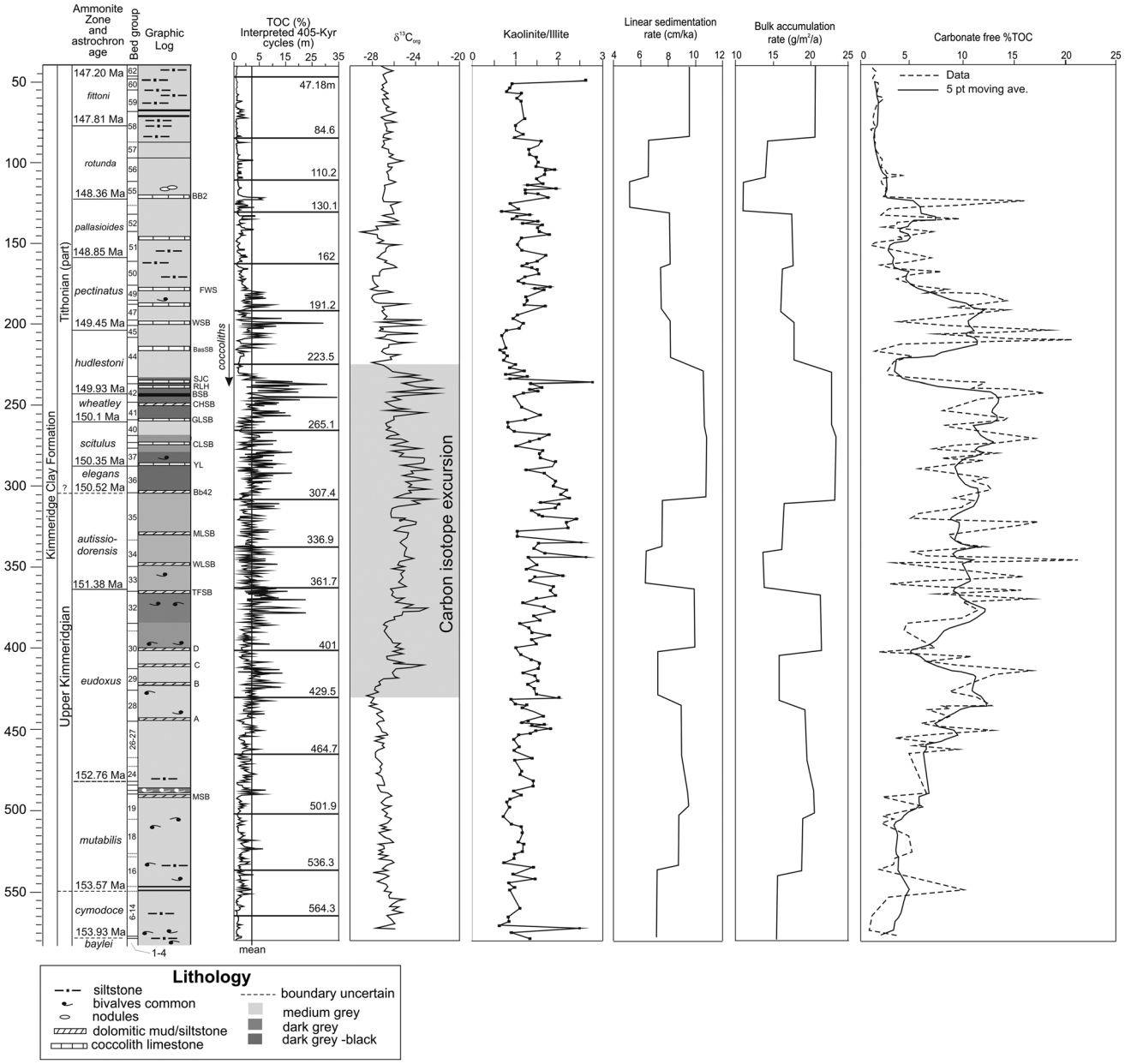

Figure 4. Conflated records of key sedimentological, climate and organic carbon burial proxy data from the Kimmeridge Clay Formation in Dorset. Chronostratigraphy, lithostratigraphy, $\delta^{13}C_{org}$, %TOC are after *Morgans-Bell et al.* [2001]; clay mineral data are from *Hesselbo et al.* [2009]. Stone Bands: BB2, Blake's Bed 2; FWS, Fresh Water Steps; WSB, White Stone Band; BaSB, Basalt; SJC, Short Joint Coal; RLH, Rope Lake head; BSB, Blackstone Band; CHSB, Clavell's Hard; GLSB, Grey Ledge; CLSB, Cattle Ledge; YL, Yellow Ledge; Bb42, Blake's Bed 42; MLSB, Maple Ledge; WLSB, Washing Ledge; TFSB, The Flats; MSB, Metherhills.

The succession above the Clavell's Hard Stone Band becomes increasingly OC-rich, with a transition from grey shales to extremely OC-rich black shales (>20% TOC) just below the Blackstone Band. The sedimentology is distinctive, with the black shales being formed of thin, event beds, with a somewhat "lenticular" fabric (Figures 5a and 5d). These lenses might be compressed ripples, bedding-parallel trace fossils, or ripped-up clasts of (microbially bound?) mud, possibly both. Burrow diameters (often >5 mm) indicates that energetic and probably oxic conditions were present at the sediment-water interface; silty, bioclastic mudstones (Figure 5b) and low-angle ripple cross-bedding (Figure 5i) also provide support for dynamic seafloor processes.

Above the Blackstone Band the %TOC remains high, but the lithology changes again, with the lower *hudlestoni* zone being marked by increasing quantities of primary carbonate from coccoliths (Figure 5c). The Rope Lake Head Stone Band and White Stone Band are coccolith limestones (Figures 5f, 5g, and 5h),

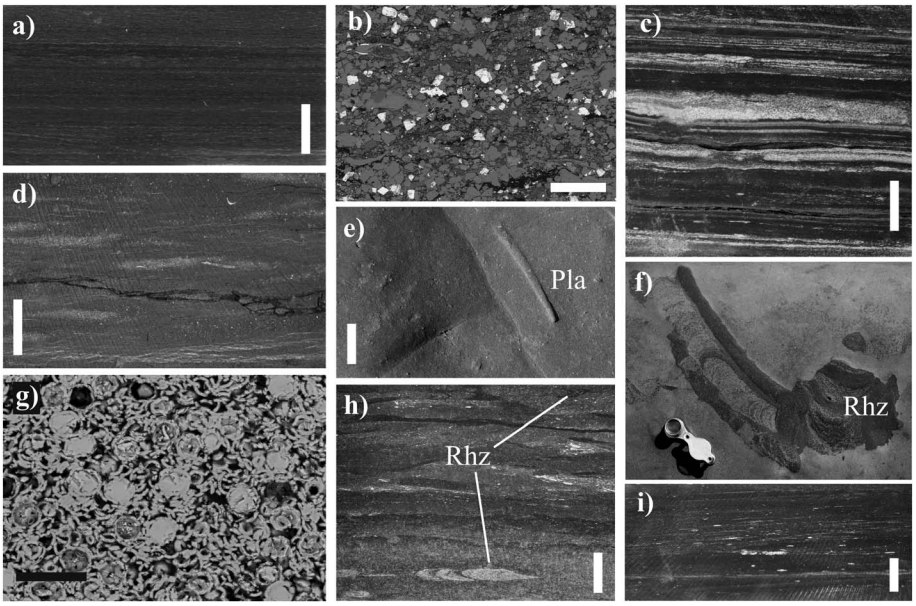

Figure 5. Sedimentary textures from the Kimmeridge Clay Formation, Kimmeridge, UK. (a) Laminated black shale; scale bar: 10 mm. (b) ESEM image of silty, bioclastic mudstone; scale bar: 80 μm. (c). Laminated, organic-rich shale and coccolith limestone; Freshwater Steps Stone Band; Swanworth Quarry borehole. (d) Fractured silty grey mudstone, 119 m depth (upper *eudoxus* zone), Metherhills borehole; scale bar: 10 mm. (e) Homogeneous (bioturbated) grey mudstone with *Planolites* (Pla) trace fossil, Clavell's Hard Stone Band (mid *wheatleyensis* zone); scale bar: 10 mm. (f) *Rhizocorallium* (Rhz) trace fossil in homogenized coccolith limestone, burrow showing spreiten formed of organic matter-rich faecal pellets; Rope Lake Head Stone Band (lower *hudlestoni* zone); hand lens: 50 mm. (g) ESEM image of coccolith limestone, White Stone Band (lower *pectinatus* zone); scale bar: 20 μm. (h) *Rhizocorallium* (Rhz)-dominated ichnofabric in coccolith limestones and black shales of White Stone Band (lower *pectinatus* zone). Note coccolith-rich spreiten in lower specimen; organic-mud-rich spreiten in upper specimen; scale bar: 10 mm. (i) Cross-laminated, organic-rich mudstones, 257.3 m depth (*wheatleyensis* zone), Swanworth Quarry borehole; scale bar: 10 mm.

rather than the dolomitic stone bands of the type present lower in the succession. The Rope Lake Head is also noticeable in containing the first large, ichnofabric-forming trace fossils: a low diversity ichnofauna dominated by faecal pellet-rich specimens of *Rhizocorallium* (Figure 5f). Burrows of this size (shaft diameter $>$10 mm) strongly support oxic conditions at the sediment-water interface, at least periodically, and are also seen in the White Stone Band (Figure 5h). The low diversity of trace makers, however, suggests that other restricting factors were present. The occurrence of grey shales homogenized by small infauna, black shales deposited as event beds, and OC-rich coccolith limestones colonized by specialized deposit-feeders are indicative of a more dynamic dysoxic-oxic environment. Our observations are consistent with those of *Wignall* [1991] who reported the upper dysaerobic biofacies contained a moderately diverse, untiered assemblage with *Rhizocorallium* and *Chrondrites*, developed in a surface mixed layer.

Figure 6 shows a stratigraphical crossplot between "basin-centered" sections in Dorset and Yorkshire and the more proximal, shoreface section at Boulonnais, northern France. Notably, high-resolution correlations of individual %TOC peaks can confidently be made between Dorset and Yorkshire, over a distance of ~400 km; they cannot be made to the Boulonnais section in northern France.

A multiproxy record with a pronounced cyclicity has been obtained from the Swanworth and Metherhills cores from the Wessex Basin [*Weedon et al*., 2004]. These records were further refined and tuned to the 405 kyr and 100 kyr eccentricity signals [*Huang et al*., 2010]. *Huang et al.* [2010] identified a hierarchy of cycles in both untuned and tuned (at 405 kyr) %TOC and Formation Micro-Scanner data throughout the formation. Their analysis showed the ~2 Myr (~167 m), ~405 Kyr (~40 m), and ~100 Kyr (9–18 m) eccentricity; ~40 Kyr obliquity (2.3–4.8 m); and ~20 Kyr precession (1.25–1.62 m) cycles.

4.3. Linear Sedimentation Rate

On average, LSRs are high, on the order of about 6 cm/kyr to 11 cm/kyr (Figure 4). The general pattern indicates the presence of a lower but irregular frequency rhythm being superimposed on the well-developed

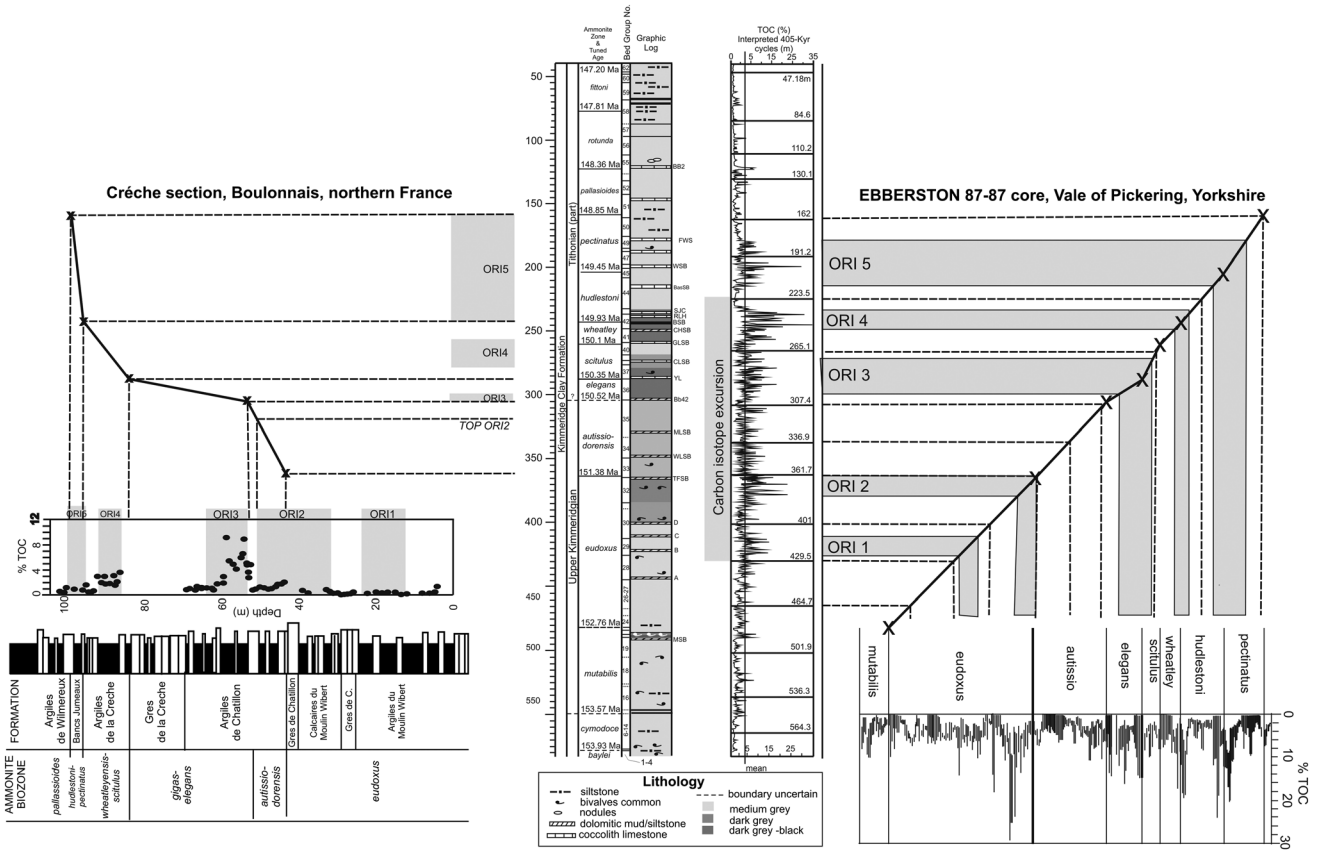

Figure 6. Stratigraphical crossplot of the type Kimmeridge Clay in Dorset [*Morgans-Bell et al.*, 2001], Yorkshire (right: Ebberston 87 core after *Herbin et al.* [1991]) and Boulonnais (left; Créche section, redrawn after *Tribvollard et al.* [2006]). Creche section is simplified to black shales, and the white boxes are shoreface sandstones. Stratigraphical scales are in meters. Organic-rich intervals (1–5) as defined by *Herbin et al.* [1991].

bed-set cycles. This rhythm is independent of the other parameters and therefore attributable to local factors including topography, bottom water currents, storm activity, and sediment grain size.

4.4. Mass Accumulation Rates

Organic matter in the KCF is dominated by Type II marine amorphous kerogen with minor Types I and III [*Farrimond et al.*, 1984; *Scotchman*, 1991]. Type III kerogen, though generally rare, is most abundant in basin margin settings, while Type II kerogens were restricted to basin centres. Hydrogen indices vary between ~120 and 550 mgHC/gTOC [*Tyson*, 2004] and are lower in proximity to the inferred paleo-shoreline and higher in more distal settings [*Scotchman*, 1991]. The section containing the highest %TOC is characterized by a positive $\delta^{13}C_{org}$ excursion that spans the *eudoxus* to mid-*hudlestoni* zones. This interval has an average >5 wt % TOC [*Morgans-Bell et al.*, 2001] (Figure 4).

OC burial and %TOC carbonate-free are both high for the Kimmeridge section and show similar patterns (Figure 4). Both increase from low values from the base of the section up to the middle of the *hudlestoni* zone. They fall back within the lower *hudlestoni* zone but then rise through the remaining *hudlestoni* to mid-*pectinatus* zone. Above the mid-*pectinatus* zone there is a gradual decline back to low values at the top of the section. Superimposed on the long-term trend are distinct higher-frequency and high-amplitude fluctuations, both parameters (Figure 4). Fluctuations in TOC are observed on ~40 m to submillimeter long cycle scales. These amplitudes are generally higher from the *eudoxus* to mid-*hudlestoni* zones.

For much of the record, periods of maximum OC burial and kaolinite/illite ratio are structured into bundles of four peaks per 400 kyr cycle (Figure 7). Based on the age model for the KCF this suggests an assigned frequency of 100 kyr for each of these peaks, and therefore, these likely reflect short eccentricity fluctuations

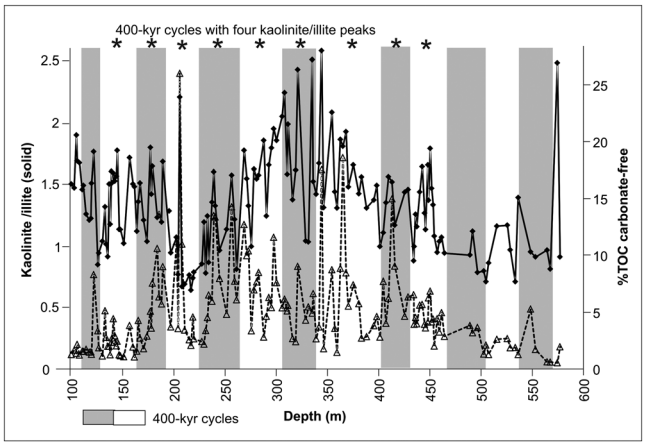

Figure 7. Relationship between kaolinite/illite and %TOC carbonate-free over depth. The 400 kyr cycles are as defined by *Huang et al.* [2010].

in climate and OC MAR. Higher-frequency fluctuations at the obliquity and precessional orbital bands are not resolved in the proxy records.

4.5. Continental Climate

In addition to the orbital-scale fluctuations there are clear longer-term trends in the kaolinite/illite record from the Dorset section [*Hesselbo et al.*, 2009] (Figures 4 and 7). The record shows an increase in the ratio from 1 in the *cymodoce* zone to a peak of 2.6 in the mid-*autissiodorensis* zone. This is followed by a decline back to a value of 1 at the top of the *hudlestoni* zone and a further rise to 2 in the *rotunda* zone.

5. Discussion

Our new climate simulations indicate a poleward shift to around ~35–40°N of high precipitation tropical-like regions, associated with changes in the Hadley circulation during the Late Jurassic greenhouse, likely driven by the clustered distribution of landmasses surrounding the proto North Atlantic and western Tethys region and topographic effects from mountain ranges along the coastlines of North America and North Africa, and along the Boreal Seaway. This climate scenario would be consistent with storm-influenced sedimentation via intensification of tropical storm tracks in a shallow water setting. Sedimentary textures indeed indicate that storms had a significant influence on sedimentation during the most OC-rich parts of the KCF. This is consistent with a variety of storm-produced event beds described from the KCF, including horizons of graded rip-up clasts, silt laminae, thin graded mud horizons, and shell pavements [*Wignall*, 1989]. A mechanism of storm-induced benthic oxygenation and temperature-stratified inhibition of storm mixing has been proposed for the abrupt nature of the decimeter-scale organic-rich and organic-lean shales in the KCF [*Wignall*, 1989].

The kaolinite/illite ratio is a well-established proxy for continental climate and associated land surface processes. Kaolinite commonly forms in soils under tropical humid conditions [*Thiry*, 2000]. In shelf basins, where riverine input of clay minerals is highest and often rapid, lateral transport of the mineral load occurs primarily with strong surface currents and during storm events, preserving an almost direct record of continental climate [*Singer*, 1984]. An alternative, diagenetic origin for the kaolinite in the KCF has been rejected based on petrography and regional considerations [*Hesselbo et al.*, 2009]. Burial maturation in the Kimmeridge Clay is also compatible with the occurrence of smectite, which is only rarely deposited in the Wessex and Cleveland basins [*Hesselbo et al.*, 2009]. Figure 7 shows the relationship between kaolinite/illite ratio and %TOC carbonate-free records as indicators of wet/dry conditions and OC burial respectively. Superimposed on the long-term (million year) trend are distinct higher-frequency and high-amplitude fluctuations at ~40 m and ~10 m scales. These high-amplitude and short-term variations occurred synchronously for TOC carbonate-free (and %TOC) and kaolinite/illite ratio on a sample-by-sample basis. Based on a mean LSR of 8.25 cm/ka, these equate with the 405 kyr and 100 kyr eccentricity cycles.

The consistency of this variability in OC MAR and kaolinite/illite ratio in these orbital power bands strongly supports a close link to climate forcing. Sedimentation, as indicated by bulk accumulation and carbonate accumulation rates in the British sector during the KCF, however, did not react in a strictly uniform manner to these orbital climate variations, which we attribute to local effects of topography, currents, sediment grain size, and/or productivity.

%TOC peak to peak correlation between the Swanworth core in Dorset and the Ebberston 87 core in Yorkshire indicate this situation extended over a distance of 400 km. The principle mechanisms responsible for these distinct patterns are hypothesized to be variations in marine productivity followed by

stratification-driven anoxia. Furthermore, OC burial and black shale formation must have been intimately linked to climate-modulated fluctuations in nutrient cycling. The supply of clay minerals from continental sources suggests continental runoff as a primary mechanism controlling nutrient supply, and thus black shale formation, consistent with organo-mineral studies of Cretaceous open marine oceanic anoxic event (OAE) black shale sections [*Kennedy and Wagner*, 2011; *Loehr and Kennedy*, 2014].

This conclusion is expected from the geological context, as the close vicinity of the Boreal Seaway to the Euro-American continent and the warm global climate during the late-Jurassic should have stimulated an intensified hydrological cycle with high precipitation and runoff [*Sellwood and Valdes*, 2008].

Orbital-scale variations in OC content are well known for marine black shales from numerous geological periods. They have been related to (1) increased OC flux to the seafloor induced by productivity pulses, (2) climate-induced variations in organic productivity, coupled with variations in bottom water redox [*Sælen et al*., 2000, and references therein], (3) water column stratification [*Tyson et al*., 1979], and (4) climate controlled production of expandable clay minerals (smectite-type) into oxygen depleted continental margin settings, catalyzing OC burial via organo-mineral interactions [*Kennedy and Wagner*, 2011].

Following the conceptual model for the Cretaceous, enhanced runoff would have promoted the establishment of anoxia/ euxinia and black shale formation along the Boreal Seaway through enhanced marine productivity. Conversely, reduced runoff would have resulted in reduced nutrient flux and marine productivity and thus partial re-establishment of oxic conditions in the water column. As demonstrated by the climate model such a situation would correspond to a more northerly position of the Intertropical Convergence Zone (ITCZ) during the late Jurassic. There is a remarkable consistency between the evidence deduced from the climate modeling and the sedimentological record across the British sector. This leads us to suggest that OC burial and black shale deposition in the KCF were intimately linked to precipitation changes that can be associated with orbital time scale fluctuations in the atmospheric circulation, and in particular changes in the extent of the Hadley cells.

Our alternative interpretation of prevailing climatic conditions in the southern part of the Late Jurassic Boreal Seaway implies a maximum reach of the ITCZ as far north as ~35°N. Such a scenario recognizes the substantially wider latitudinal shift of the ITCZ in the modern Pacific region compared to the Atlantic region, with the ITCZ migrating seasonally over ~60° of latitude and a maximum northern position at ~35°N during boreal summer. Identification of the outer subtropical boundary hints toward a low-latitude influence on marine sedimentation and OC burial in the Arctic sector of the Boreal Seaway. *Mutterlose et al*. [2003] reported OC-rich Kimmeridgian-Tithonian aged shales as far north as the Barents Sea (54°N in the Late Jurassic), with sedimentary cycles containing a distinct precessional-pacing, consistent with some influence from low-latitude fluctuations in insolation. In the late Jurassic the northern Hadley cell may therefore have extended, at least temporarily, imposing dynamic, subtropical conditions close to the paleo-Arctic.

We therefore propose that orbital forcing in the Late Jurassic would have controlled alternations between extremely humid conditions, supporting peak OC burial in the KCF, and dryer periods where freshwater supply and redox conditions relaxed, resulting in lower OC burial. A depositional system with strongly alternating hydrological conditions is consistent with many black shales from the Cretaceous Oceanic Anoxic Events [*Wagner et al.,* 2013; *Beckmann et al*., 2005] and the Neogene Mediterranean sapropels [*Rossignol-Strick*, 1985].

The onset of a drier climate in the upper Tithonian of the British sector may indicate a gradual transition to a more subtropical climate with stronger trade winds. The underlying mechanism for this large-scale shift in climate conditions remains unclear, but a link to the long-term and global scale drawdown of CO_2 during peak Kimmeridgian black shale deposition has been proposed [see also *Wignall and Ruffell*, 1990]. These conditions would have promoted global cooling and eventually incipient glaciation [*Donnadieu et al*., 2011]. The emergence of incipient south polar ice sheets in the later Tithonian should has led to an increase in global surface meridional temperature gradient and a contraction of the outer boundaries of the Hadley cells, gradually shifting the British KCF out of the direct influence of tropical and eventually also subtropical climate conditions.

6. Conclusions

The Kimmerdige black shales from the late Jurassic epeiric Boreal Seaway were deposited at high average sedimentation rates (8 cm/kyr) enabling the investigation of paleoclimate and paleoceanography at high temporal resolution and associated hydrocarbon source-rock formation. The KCF was deposited between

~35°N and ~65°N in temperature- or salinity-stratified subbasins. Deposition was strongly influenced by frequent storm activity and high rates of sedimentation leading to expanded shale sections and massive burial of organic matter. Analyses of the relationships between clay mineral assemblages (kaolinite/illite) and OC content support the conclusion that changes in OC burial resulted from orbitally paced fluctuation in rainfall intensity beneath the ascending limb of the Hadley cell, i.e., under the direct influence of the tropical ITCZ. Our new climate simulations support this tropical scenario. Together, these suggest that the variable but overall very high burial of OC in the KCF was controlled by very similar mechanisms as some of the Cretaceous OAE's and the Mediterranean sapropels.

The implications of this reinterpretation of high-resolution records from Dorset and Yorkshire for temperate and subpolar depositional settings in the Late Jurassic are yet unclear. These may have been profound, affecting the location of frontal systems, runoff patterns, salinity stratification, and gradients in sea surface temperature and seawater redox. Additional high-resolution records from the northern Boreal Seaway and the proto-Arctic combined with model simulations incorporating orbital variability explicitly are needed to validate and constrain the wider implications of the Jurassic model proposed in this study.

Acknowledgments

Funding was provided by NERC Oil and Gas Catalyst grant (NE/L008092/1) and the Durham University PVC Research Seedcorn Fund. D.J.L. and A.F. acknowledge NERC grant NE/K014757/1. The geologic data used in this analysis were collected as part of the Natural Environment Research Council's Rapid Global Geological Events special topic "Anatomy of a Source Rock" and is open access at www.earth.ox.ac.uk/~rgge/data.html. We acknowledge fruitful discussions with many colleagues, particularly J. Trabucho-Alexandre and R.V. Tyson. Lauren Raynham and Amanda Galsworthy from the "Getech Globe" paleogeographic mapping team were essential in producing the basemaps used in this study. The helpful comments of the anonymous referees and editor significantly improved this paper. Supporting information can be found in the supplementary files and figures.

References

Arthur, M. A., and B. B. Sageman (1994), Marine black shales: Depositional mechanisms and environments of ancient deposits, *Annu. Rev. Earth Planet. Sci.*, *22*, 499–551.

Beckmann, B., T. Wagner, and P. Hofmann (2005), Linking Coniacian-Santonian (OAE3) black shale deposition to African climate variability: A reference section from the eastern tropical Atlantic at orbital timescales (ODP site 959, Off Ivory Coast and Ghana), *SEPM Spec. Publ.*, *82*, 125–143.

Berger, A., J. Imbrie, J. Hays, G. Kukla, and B. Saltzman (1984), *Milankovitch and Climate. Understanding the Response to Orbital Forcing*, D. Reidel, Amsterdam.

Berry, G., and M. J. Reeder (2014), Objective identification of the intertropical convergence zone: Climatology and trends from the ERA-Interim, *J. Clim.*, *27*(5), 1894–1909.

Dera, G., B. Brigaud, F. Monna, R. Laffont, E. Pucéat, J.-F. Deconinck, P. Pellenard, M. M. Joachimski, and C. Durlet (2011), Climatic ups and downs in a disturbed Jurassic world, *Geology*, *39*(3), 215–218.

Desprairies, A., M. Bachaoui, A. Ramdani, and N.-P. Tribovillard (1995), Clay diagenesis in organic-rich cycles from the Kimmeridge Clay Formation of Yorshire (G.B.): implication for palaeoclimatic interpretations, in *The Organic Cyclicities of the Kimmeridge Clay Formation (Yorkshire, GB) and the Recent Maar Sediments (Lac du Bouchet, France). Lecture Notes in Earth Sciences*, pp. 63–91, edited by E. Lallier-Verges, N.-P. Tribovillard, and P. Bertrand, Springer, Berlin.

Donnadieu, Y., G. Dromart, Y. Goddéris, E. Pucéat, B. Brigaud, G. Dera, C. Dumas, and N. Olivier (2011), A mechanism for brief glacial episodes in the Mesozoic greenhouse, *Paleoceanography*, *26*, PA3212, doi:10.1029/2010PA002100.

Farrimond, P., P. Comet, G. Eglinton, R. P. Evershed, M. A. Hall, D. W. Park, and A. M. Wardroper (1984), Organic geochemical study of the Upper Kimmeridge Clay of the Dorset type area, *Mar. Pet. Geol.*, *1*(4), 340–354.

Getech (2013), Atlases of Global Palaeogeography - Jurassic.

Hay, W., R. DeConto, and S. Flögel (2013), Cretaceous continental hydrology–Different from today, *Earth Sci. Rev.*, *115*(4), 262–272.

Herbin, J.-P., C. Muller, J. Geyssant, F. Melieres, and I. Penn (1991), Hétérogénéité quantitative et qualitative de la matiére organique dand les argiles du Kimméridgien du Val de Pickering (Yorkshire, UK): cadre sédimentologique et stratigraphique, *Rev. Institut Fr. Pétrol.*, *46*(6), 675–712.

Hesselbo, S. P., J.-F. Deconnick, J. M. Huggett, and H. S. Morgans-Bell (2009), Late Jurassic palaeoclimatic change from clay mineralogy and gamma-ray spectrometry of the Kimmeridge Clay, Dorset, UK, *J. Geol. Soc.*, *166*(6), 1123–1133.

Hofmann, P., and T. Wagner (2011), ITCZ controls on Late Cretaceous black shale sedimentation in the tropical Atlantic Ocean, *Paleoceanography*, *26*, PA002154, doi:10.1029/2011PA002154.

Huang, C., S. P. Hesselbo, and L. Hinnov (2010), Astrochronology of the late Jurassic Kimmeridge Clay (Dorset, England) and implications for Earth system processes, *Earth Planet. Sci. Lett.*, *289*(1–2), 242–255.

Jenkyns, H. C. (1980), Cretaceous anoxic events: From continents to oceans, *J. Geol. Soc.*, *137*, 171–188.

Jenkyns, H. C. (2003), Evidence for rapid climate change in the Mesozoic-Palaeogene greenhouse world, *Philos. Trans. R. Soc. London, Ser. A*, *361*(1810), 1885–1916.

Kennedy, M. J., and T. Wagner (2011), Clay mineral continental amplifier for marine carbon sequestration in a greenhouse ocean, *Proc. Natl. Acad. Sci. U.S.A.*, *108*(24), 9776–9781.

Kuhnt, W., F. Luderer, S. Nederbragt, J. Thurow, and T. Wagner (2005), Orbital-scale record of the late Cenomanian-Turonian oceanic anoxic event (OAE-2) in the Tarfaya Basin (Morocco), *Int. J. Earth Sci.*, *94*(1), 147–159.

Löhr, S. C., and M. J. Kennedy (2014), Organomineral nanocomposite carbon burial during Oceanic Anoxic Event 2, *Biogeosciences*, *11*, 4971–4983.

Lunt, D. J., A. Farnsworth, C. Loptson, G. L. Foster, P. Markwick, C. L. O'Brien, R. D. Pancost, S. A. Robinson, and N. Wrobel (2016), Palaeogeographic controls on climate and proxy interpretation, *Clim. Past*, *12*, 1181–1198, doi:10.5194/cp-12-1181-2016.

Macquaker, J., and R. Gawthorpe (1993), Mudstone lithofacies in the Kimmeridge Clay Formation, Wessex Basin, southern England: Implications for the origin and controls of the distribution of mudstones, *J. Sediment. Res.*, *63*(6), 1129–1143.

Manabe, S., and K. Bryan (1985), CO_2-induced change in a coupled ocean-atmosphere model and its paleoclimatic implications, *J. Geophys. Res.*, *90*, 11,689–11,707, doi:10.1029/JC090iC06p11689.

Markwick, P. J., and P. J. Valdes (2004), Palaeo-digital elevation models for use as boundary conditions in coupled ocean-atmosphere GCM experiments: A Maastrichtian (late Cretaceous) example, *Palaeogeogr. Palaeoclimatol. Palaeoecol.*, *213*(1), 37–63.

Morgans-Bell, H. S., A. L. Coe, S. P. Hesselbo, H. C. Jenkyns, G. P. Weedon, J. E. A. Marshall, R. V. Tyson, and C. J. Williams (2001), Intergrated stratigraphy of the Kimmerdige Clay Formation (Upper Jurassic) based on exposures and boreholes in south Dorset, UK, *Geol. Mag.*, *138*, 511–539.

Mutterlose, J., H. Brumsack, S. Flögel, W. Hay, C. Klein, U. Langrock, M. Lipinski, W. Ricken, E. Söding, and R. Stein (2003), The Greenland-Norwegian Seaway: A key area for understanding Late Jurassic to Early Cretaceous paleoenvironments, *Paleoceanography*, *18*(1), 1010, doi:10.1029/2001PA000625.

Ohba, M., and H. Ueda (2010), A GCM study on effects of continental drift on tropical climate at the Early and Late Cretaceous, *J. Meteorol. Soc. Jpn.*, *88*(6), 869–881.

Oschmann, W. (1991), Distribution, dynamics and palaeoecology of Kimmeridgian (Upper Jurassic) shelf anoxia in western Europe, in *Modern and Ancient Continental Shelf Anoxia*, edited by R. V. Tyson and T. H. Pearson, *Geol. Soc. London, Spec. Publ.*, 381–395.

Rossignol-Strick, M. (1985), Mediterranean Quaternary sapropels, an immediate response of the African monsoon to variation of insolation, *Palaeogeogr. Palaeoclimatol. Palaeoecol.*, *49*(3), 237–263.

Sælen, G., R. Tyson, N. Telnæs, and M. Talbot (2000), Contrasting watermass conditions during deposition of the Whitby Mudstone (Lower Jurassic) and Kimmeridge Clay (Upper Jurassic) formations, UK, *Palaeogeogr. Palaeoclimatol. Palaeoecol.*, *163*(3), 163–196.

Scotchman, I. C. (1991), Kerogen facies and maturity of the Kimmeridge Clay Formation in southern and eastern England, *Mar. Pet. Geol.*, *8*, 278–295.

Sellwood, B. W., and P. J. Valdes (2008), Jurassic climates, *Proc. Geologists' Assoc.*, *119*(1), 5–17.

Singer, A. (1984), The paleoclimatic interpretation of clay minerals in sediments—A review, *Earth Sci. Rev.*, *21*(4), 251–293.

Thiry, M. (2000), Palaeoclimatic interpretation of clay minerals in marine deposits: An outlook from the continental origin, *Earth Sci. Rev.*, *49*(1), 201–221.

Tribvollard, N., T. J. Algeo, T. W. Lyons, and A. Riboulleau (2006), Trace metals as paleoredox and paleoproductivity proxies: An update, *Chem. Geol.*, *232*, 12–32.

Tyson, R. (2001), Sedimentation rate, dilution, preservation and total organic carbon: Some results of a modelling study, *Org. Geochem.*, *32*(2), 333–339.

Tyson, R. V. (1996), Sequence-stratigraphical interpretation of organic facies variations in marine siliciclastic systems: General principles and application to the onshore Kimmeridge Clay Formation, UK, in *Sequence stratigraphy in British Geology*, edited by S. P. Hesselbo and D. N. Parkinson, *Geol. Soc. London, Spec. Publ.*, 103, 75–96.

Tyson, R. V. (2004), Variation in marine total organic carbon through the type Kimmeridge Clay Formation (Late Jurassic), Dorset, UK, *J. Geol. Soc.*, *161*(4), 667–673.

Tyson, R. V., R. C. L. Wilson, and C. Downie (1979), A stratified water column model for the type Kimmeridge Clay, *Nature*, *277*, 377–380.

Van Kaam-Peters, H. M., S. Schouten, J. Köster, and J. S. S. Damstè (1998), Controls on the molecular and carbon isotopic composition of organic matter deposited in a Kimmeridgian euxinic shelf sea: Evidence for preservation of carbohydrates through sulfurisation, *Geochim. Cosmochim. Acta*, *62*(19), 3259–3283.

Wagner, T., P. Hofmann, and S. Flögel (2013), Marine black shale deposition and Hadley cell dynamics: A conceptual framework for the Cretaceous Atlantic Ocean, *Mar. Pet. Geol.*, *43*, 222–238.

Wang, W., P. Xie, S.-H. Yoo, Y. Xue, A. Kumar, and X. Wu (2011), An assessment of the surface climate in the NCEP climate forecast system reanalysis, *Clim. Dyn.*, *37*(7–8), 1601–1620.

Weedon, G. P., A. L. Coe, and R. W. Gallois (2004), Cyclostratigraphy, orbital tuning and inferred productivity for the type Kimmeridge Clay (Late Jurassic), Southern England, *J. Geol. Soc.*, *161*, 655–666.

Wignall, P. B. (1989), Sedimentary dynamics of the Kimmeridge Clay: Tempests and earthquakes, *J. Geol. Soc.*, *146*(2), 273–284.

Wignall, P. B. (1991), Dysaerobic trace fossils and ichnofabrics in the Upper Jurassic Kimmeridge Clay of Southern England, *Palaios*, *6*(3), 264–270.

Wignall, P. B., and A. H. Ruffell (1990), The influence of a sudden climatic change on marine deposition in the Kimmeridgian of northwest Europe, *J. Geol. Soc.*, *147*(2), 365–371.

Yin, J. H. (2005), A consistent poleward shift of the storm tracks in simulations of 21st century climate, *Geophys. Res. Lett.*, *32*, L18701, doi:10.1029/2005GL023684.